

Structure and Dynamics of Acetonitrile at the Air/Liquid Interface of Binary Solutions Studied by Infrared–Visible Sum Frequency Generation

Joonyeong Kim, Keng C. Chou, and Gabor A. Somorjai*

Department of Chemistry, University of California at Berkeley, Berkeley, California 94720, and Materials Sciences Division, Lawrence Berkeley National Laboratory, Berkeley, California 94720

Received: May 16, 2002; In Final Form: August 21, 2002

Infrared–visible sum frequency generation (SFG) vibrational spectroscopy was employed to investigate the molecular level details of acetonitrile (CH_3CN) structure at the air/liquid interface of binary solutions with *per*-deuterated acetonitrile (CD_3CN), water, and carbon tetrachloride (CCl_4). In the case of the CH_3CN – CD_3CN system, the SFG signal intensity for the symmetric CH stretch ($\text{CH}(\text{s})$) mode increases proportionally with the bulk mole fraction of CH_3CN ($x_{\text{CH}_3\text{CN}}$). However, the SFG signal intensity of the $\text{CH}(\text{s})$ mode from the CH_3CN –water system is rapidly enhanced, reaches a maximum, and gradually attenuates as $x_{\text{CH}_3\text{CN}}$ is varied from 0 to 1. Mixtures of CH_3CN and CCl_4 generally exhibit less SFG intensity for the $\text{CH}(\text{s})$ mode compared to the CH_3CN – CD_3CN and CH_3CN –water systems for a corresponding $x_{\text{CH}_3\text{CN}}$. For quantitative analysis, the contributions to the SFG signal intensity were separated into the orientation factor and surface number density. As a consequence, it was found that CH_3CN molecules in the CH_3CN – CD_3CN mixtures exhibit a concentration-independent orientation similar to those in neat CH_3CN . For the CH_3CN –water system, CH_3CN molecules become less tilted with respect to the surface normal and more ordered than those in neat CH_3CN by lowering $x_{\text{CH}_3\text{CN}}$. In contrast, CH_3CN molecules in the CH_3CN – CCl_4 system are generally less ordered and more tilted with respect to the surface normal compared to the case of neat CH_3CN .

Introduction

The structure and dynamics of molecules at the air/liquid interface has been a subject of extensive research because of its importance in fundamental science and potential applications in wetting, lithography, atmospheric and environmental chemistry, photochemistry, and thin film formation.^{1–5} Many experimental and theoretical studies have revealed that molecules adopt a preferred orientation at the air/liquid interface, which is significantly different from the bulk solution where most molecules are randomly and isotropically distributed.^{1–3} Despite our progress in understanding molecular properties at the interface, obtaining detailed structural information has represented a considerable experimental challenge. This is partly due to the lack of proper probing techniques that are exclusively sensitive to molecules on surfaces or interfaces.

For the past decade, infrared–visible sum frequency generation (SFG) vibrational spectroscopy has proven to be a powerful technique to probe molecular structures at various interfaces.^{3,6–11} As a second-order nonlinear optical process, SFG is forbidden in media that possess bulk inversion symmetry but is allowed at interfaces or surfaces where inversion symmetry is broken. This technique, therefore, can be employed as an interface- or surface-specific probe for systems, even in the presence of an overwhelming bulk contribution.

Previous infrared–visible SFG studies in the CN stretch region have shown that CH_3CN molecules at the air/liquid interface of the CH_3CN –water system exhibit abrupt structural changes by varying bulk composition.^{12–14} Hydrogen bonding between CH_3CN and water is known to significantly affect the structure of interfacial CH_3CN molecules. In this paper, SFG spectra in the CH stretch region have been monitored to investigate the structure and dynamics of CH_3CN molecules at

the air/liquid interface of various binary mixtures with different bulk CH_3CN concentrations. We prepared binary CH_3CN solutions with and without hydrogen bonding by the use of water and carbon tetrachloride (CCl_4), respectively. Binary mixtures of CH_3CN and *per*-deuterated acetonitrile (CD_3CN) were also studied as a reference because the orientation and ordering of CH_3CN in this mixture is assumed to be similar over the composition range.

Our SFG results revealed that the structure of interfacial CH_3CN molecules is intimately affected by the nature and composition of the coexisting component in the binary mixtures. Namely, interfacial CH_3CN molecules in the CH_3CN –water system show better ordering compared with the CH_3CN – CCl_4 and CH_3CN – CD_3CN systems.

Experimental Section

SFG. The theory and experimental setup of SFG have been described in detail elsewhere.^{15,16} Briefly, infrared–visible SFG vibrational spectroscopy involves a second-order nonlinear optical process in which two input beams, with frequencies ω_{ir} and ω_{vis} , overlap in a medium to generate an output beam at the sum frequency, ω_{sfg} . The intensity of the SFG signal, I_{sfg} , is proportional to the square of the surface nonlinear susceptibility:

$$I_{\text{sfg}} \propto |\chi_{\text{NR}}^{(2)} + \chi_{\text{R}}^{(2)}|^2 = |\chi_{\text{NR}}^{(2)} + \sum_q \frac{A_q}{\omega_{\text{IR}} - \omega_q + i\Gamma}|^2 \quad (1)$$

with

$$A_{q,ijk} = n \sum_{lmn} a_{q,lmn} \langle (\hat{i} \cdot \hat{l})(\hat{j} \cdot \hat{m})(\hat{k} \cdot \hat{n}) \rangle \quad (2)$$

$$a_{q,lmn} = -\frac{1}{2\epsilon_0\omega_q} \frac{\partial \mu_n}{\partial Q_q} \frac{\partial \alpha_{lm}}{\partial Q_q} \quad (3)$$

* To whom correspondence should be addressed. Tel: 510-642-4053. Fax: 510-643-9668. E-mail: somorjai@socrates.berkeley.edu.

where $\chi_{\text{NR}}^{(2)}$, $\chi_{\text{R}}^{(2)}$, A_{q} , ω_{q} , Γ , $\langle \rangle$, μ_n , and α_{lm} are the nonresonant contribution, resonant contribution, oscillator strength, resonant frequency, width, average over orientation distribution, infrared dipole, and Raman tensor, respectively. The oscillator strength, A_{q} , is related to $a_{\text{q},lm}$, the number density of contributing oscillators, n , and an orientation-averaged coordinate transformation. In eq 3, $a_{\text{q},lm}$ is interpreted as the product of derivatives of both the polarizability and dipole and gives the constraint that the vibrational mode must be both infrared- and Raman-active for a sum frequency signal to be resonantly enhanced. SFG spectra were collected using the $s_{\text{sfg}}s_{\text{vis}}p_{\text{ir}}$ polarization combination (*ssp*), which specifically probes the yyz component of A_{q} , a 27-component tensor. Additional spectra were collected using the $s_{\text{sfg}}p_{\text{vis}}s_{\text{ir}}$ polarization combination (*sps*), which is sensitive to the zyz component of A_{q} .

Laser System and Data Collection. SFG spectra were obtained with a passive-active mode-locked Nd:YAG laser (PY61, Continuum, Santa Clara, CA). The 1064 nm light generated has a pulse width of 20 ps, and the laser operates at a 20 Hz repetition rate. Radiation is sent to an optical parametric generator/amplifier (OPG/OPA) stage (Laser Vision, Bellevue, WA) where tunable infrared radiation is produced in addition to frequency-doubled radiation at 532 nm. The OPG/OPA consists of two parts. The first is an angle-tuned potassium titanyl phosphate (KTP) stage pumped with 532 nm light to generate near-infrared radiation between 1.35 and 1.85 μm . This output is then mixed with the 1064 nm fundamental in an angle-tunable potassium titanyl arsenate (KTA) stage to produce a tunable infrared beam from 2000 to 4000 cm^{-1} (7 cm^{-1} fwhm). The tunable infrared beam is overlapped with the 532 nm radiation at the sample interface at incident angles of 51° and 42° , respectively, with respect to the surface normal. The SFG signal generated from the sample is collected by a photomultiplier tube, sent to a gated integrator, and recorded digitally. For each scan, data is collected with 200 shots per data point in 5 cm^{-1} increments in the 2850–3050 cm^{-1} range and normalized by infrared beam intensity measured at the sample stage. For a given condition, SFG measurements were repeated at least three times and data were averaged to produce the final spectra presented in this paper. The frequency of the infrared beam was calibrated to $\pm 2 \text{ cm}^{-1}$ by the use of a polystyrene standard absorption spectra.

The effect of laser heating was investigated by solving a heat diffusion equation. The IR beam has an intensity of 300 μJ with a spot diameter of 1.0 mm at the air/liquid interface. Because the absorption coefficient of water and acetonitrile is about 1000 and 350 cm^{-1} , respectively,¹⁷ in the studied frequency region, the temperature gradient in the surface normal direction is much larger than that in the direction parallel to the surface. Therefore, the heat diffusion equation was simplified to a one-dimensional equation:

$$\rho C_p \frac{\partial T(z,t)}{\partial t} = Q + k \frac{\partial^2 T(z,t)}{\partial z^2} \quad (4)$$

where ρ , C_p , Q , and k are density, heat capacity, heat added by laser, and thermal conductivity, respectively. The calculated temperature change in the liquid surface due to laser irradiation was no more than 20 $^\circ\text{C}$.

Materials. Acetonitrile (CH_3CN , >99.9%, Sigma-Aldrich Laborchemikalien GmbH), *per*-deuterated acetonitrile (CD_3CN , >99.8%, Sigma-Aldrich), and carbon tetrachloride (CCl_4 , >99.9%, Sigma-Aldrich) were used as received. The water used in the preparation of binary solutions and in the cleaning of the

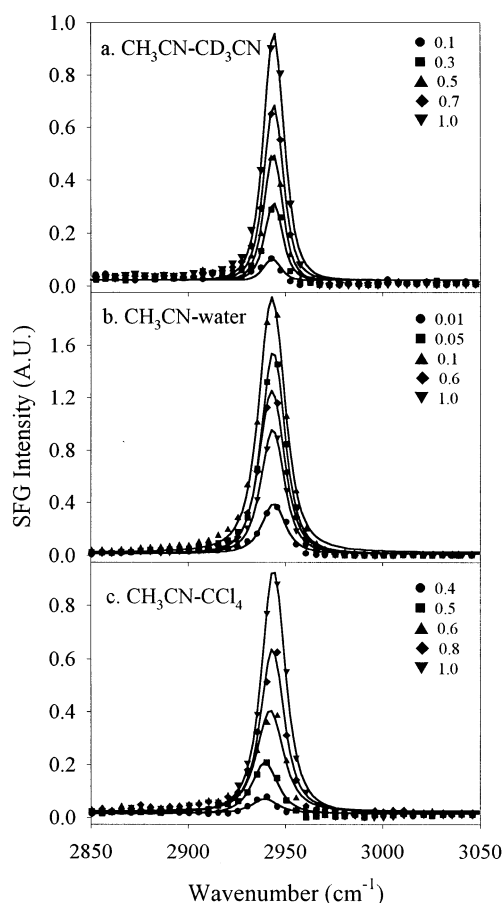


Figure 1. Representative SFG spectra at the air/liquid interfaces of binary solutions of (a) CH_3CN – CD_3CN , (b) CH_3CN –water, and (c) CH_3CN – CCl_4 . The solid lines are calculated fits to the data using eq 1. Note that the CD stretch mode for CD_3CN is located around 2120 cm^{-1} and invisible in the spectra in panel a. The beam polarization employed was *s* (sum frequency), *s* (visible input), and *p* (infrared input).

experimental apparatus was produced by a Millipore Water Purification System with a minimum resistivity of 18.0 $\text{M}\Omega\cdot\text{cm}$. Binary solutions of CH_3CN – CD_3CN , CH_3CN –water, and CH_3CN – CCl_4 were prepared by mixing appropriate amounts of liquids.

Results

SFG spectra in the CH stretch region for three binary CH_3CN – CD_3CN , CH_3CN –water, and CH_3CN – CCl_4 solutions were collected at the air/liquid interface as a function of the bulk mole fraction of CH_3CN ($x_{\text{CH}_3\text{CN}}$). Representative SFG data for each binary system are shown in Figure 1. The polarization combination used was *ssp*, with respect to SFG signal, visible input, and infrared input components. The solid lines represent least-squares fits to the raw data using eq 1. All SFG spectra contain one peak located near 2944 cm^{-1} that is assigned to the symmetric CH stretch (CH(s)) mode. No spectral features of the asymmetric CH stretch (CH(a)) mode were observed (typically around 3004 cm^{-1}). Note that the CD stretch mode for CD_3CN is located around 2120 cm^{-1} and thereby invisible in the CH stretch region (Figure 1a).^{12–14} For the CH_3CN – CD_3CN and CH_3CN – CCl_4 systems, the SFG signal intensity for the CH(s) mode increases with the bulk composition of CH_3CN (Figure 1a,c). However, SFG intensity for the CH(s) mode for the CH_3CN –water system is not proportional to bulk $x_{\text{CH}_3\text{CN}}$ (Figure 1b). The strongest peak intensity is observed when $x_{\text{CH}_3\text{CN}} \approx 0.1$ rather than from neat CH_3CN .

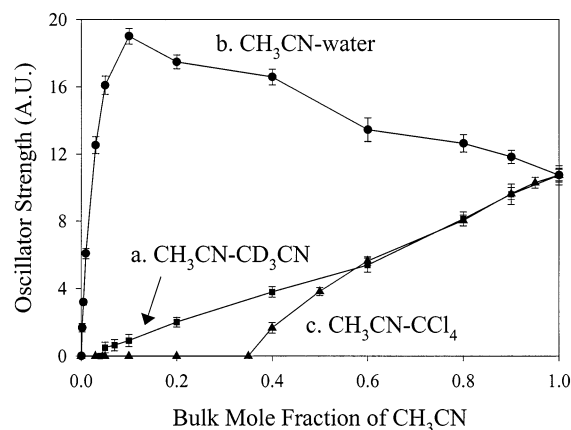


Figure 2. Oscillator strengths of the CH(s) mode near 2944 cm⁻¹ as a function of the bulk mole fraction of CH₃CN for the (a, ■) CH₃CN-CD₃CN, (b, ●) CH₃CN-water, and (c, ▲) CH₃CN-CCl₄ systems.

For quantitative data analysis, oscillator strengths (A_q in eq 1) of the CH(s) mode in the SFG spectra for the three binary solutions over various compositions of CH₃CN were obtained by fitting to eq 1 and plotted as a function of the bulk CH₃CN mole fraction, $x_{\text{CH}_3\text{CN}}$. The results are presented in Figure 2. Several features are noteworthy. First, the oscillator strength from the CH₃CN-water solutions (line b in Figure 2) is generally larger than that from the CH₃CN-CD₃CN and CH₃CN-CCl₄ systems (lines a and c in Figure 2) for a given bulk composition. This trend is more obvious at lower $x_{\text{CH}_3\text{CN}}$. Another feature found in Figure 2 is that the changes in the oscillator strength of each binary system exhibit a different dependence on the bulk concentration of CH₃CN. For the CH₃CN-CD₃CN solutions (line a in Figure 2), the oscillator strength is nearly proportional to the bulk CH₃CN composition. In the case of the CH₃CN-water system, however, the oscillator strength is dramatically enhanced, reaches its maximum around $x_{\text{CH}_3\text{CN}} = 0.1$, and gradually decreases as $x_{\text{CH}_3\text{CN}}$ is further raised (line b in Figure 2). The opposite trend is observed for the CH₃CN-CCl₄ solutions, in which the oscillator strength is rapidly attenuated and disappears when $x_{\text{CH}_3\text{CN}}$ is around 0.35 (line c in Figure 2).

According to eqs 2 and 3, the oscillator strength, A_q , is governed by the surface number density (n) and the orientation average of the product of the polarizability and dipole derivatives for a given vibrational mode. The surface compositions of the binary CH₃CN-water and CH₃CN-CCl₄ systems are, however, not simply related to the bulk compositions. Detailed procedures for obtaining the theoretical surface composition from the bulk composition by the use of experimental surface tension data are described elsewhere.¹⁸⁻²¹ Shortly, the surface composition of these binary systems can be estimated by the application of the Gibbs adsorption equation and surface tension using

$$\left(\frac{\partial\gamma}{\partial c}\right)_T = -\frac{RT\Gamma_s}{c} \quad (5)$$

where Γ_s , c , γ , R , and T are surface excess, bulk mole fraction, surface tension of the mixture, gas constant, and temperature, respectively. For an approximation, we assume that the area occupied by each species is independent of the mole fraction and estimated surface areas of 8.0, 24.0, and 25.0 Å²/molecule for water, acetonitrile, and CCl₄ were used.^{12,19,20} Experimental surface tension data for the CH₃CN-H₂O and CH₃CN-CCl₄ systems are adopted from literature.^{22,23} For the binary CH₃CN-CD₃CN system, the surface composition is considered to

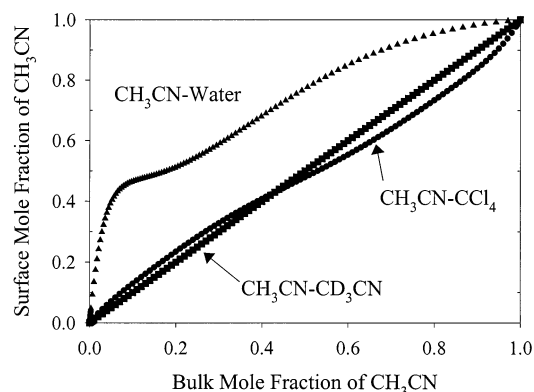


Figure 3. Estimated surface composition of CH₃CN in the (■) CH₃CN-CD₃CN, (●) CH₃CN-water, and (▲) CH₃CN-CCl₄ systems.

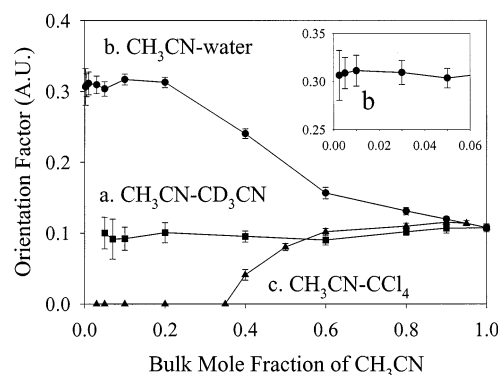


Figure 4. Orientation factor (A_q/n) from the oscillator strength and the theoretical surface composition for the (a, ■) CH₃CN-CD₃CN, (b, ●) CH₃CN-water, and (c, ▲) CH₃CN-CCl₄ systems. Inset shows the data at low bulk mole fractions of CH₃CN for the CH₃CN-water system. The greater orientation factor indicates that acetonitrile molecules are more ordered and less tilted with respect to the surface normal.

be close to the bulk composition because the two components exhibit nearly identical surface tension and molecular dimensions. In Figure 3, the estimated surface composition of CH₃CN in the binary CH₃CN-water mixture is shown to be much larger than that for the bulk composition, indicating that CH₃CN molecules preferentially aggregate at the surface. In contrast, the surface concentration of CH₃CN for the CH₃CN-CCl₄ system is comparable to the bulk concentration.

From the fitted oscillator strength (Figure 2) and estimated surface composition (Figure 3), the oscillator strength per molecule (A_q/n) of the CH(s) mode is obtained, and the results are shown in Figure 4. According to eqs 2 and 3, the oscillator strength per molecule (A_q/n) depends on the orientation average of the product of the polarizability and dipole derivatives for a given vibrational mode. The oscillator strength per molecule (A_q/n), therefore, can be regarded as an *orientation factor* for the SFG peak intensity, which provides information regarding the *ordering*, as well as the *spatial orientation*, of molecules. Under the *ssp* polarization combination, for example, a maximum orientation factor can be achieved when every molecule adopts a conformation with its vibrational dipole component (μ_n) directed along the surface normal (z) and the polarizability tensor component (α_{lm}) lying along the surface ($x-y$).²⁴⁻²⁸

In Figure 4, it is found that the orientation factor for the CH(s) mode of CH₃CN at the interface depends on the coexisting component and its concentration. For the CH₃CN-CD₃CN system, the magnitude of the orientation factor is nearly constant

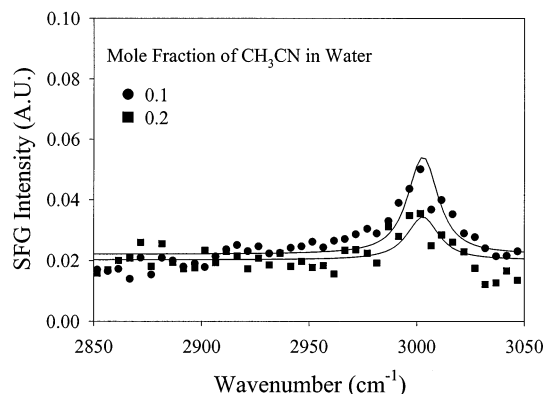


Figure 5. SFG spectra of CH₃CN at the air/liquid interfaces of the CH₃CN–water solutions with bulk molar fraction of CH₃CN at (●) 0.1 and (■) 0.2. The solid lines are calculated fits to the data using eq 1. The beam polarization employed was *s* (sum frequency), *p* (visible input), and *s* (infrared input).

over the full composition range investigated indicating that the orientation and ordering of CH₃CN molecules is concentration-independent (line a in Figure 4). However, the orientation factor from the CH₃CN–water system remains large up to $x_{\text{CH}_3\text{CN}} = 0.2$ and then attenuates as $x_{\text{CH}_3\text{CN}}$ increases further (line b in Figure 4). The opposite trend is observed for the CH₃CN–CCl₄ system, in which the orientation factor rapidly attenuates as $x_{\text{CH}_3\text{CN}}$ falls below 0.6 (line c in Figure 4).

To obtain additional structural information for CH₃CN at the interface, SFG experiments were conducted with the *sps* polarization combination. Detectable SFG signals were obtained only from the CH₃CN–water system with $x_{\text{CH}_3\text{CN}} = 0.1$ and 0.2 (see Figure 5). SFG spectra contain an exclusive peak at 3004 cm^{−1} attributed to the CH(a) mode, and no spectral features for the CH(s) mode are found. Interestingly, the bulk composition for detectable SFG spectra under the *sps* polarization condition is close to the case for which maximum SFG signal intensity of the CH(s) mode is observed with the *ssp* polarization combination. Both CH₃CN–CD₃CN and CH₃CN–CCl₄ mixtures did not produce any observable SFG signals over the full composition range.

Discussion

The difference in the concentration-dependent oscillator strengths for the three binary systems presented in Figure 2 can be explained by the surface number density and the orientation of CH₃CN at the interface. CH₃CN molecules in the CH₃CN–CD₃CN system adopt a virtually concentration-independent conformation that is similar to neat CH₃CN, as indicated by the nearly comparable orientation factor in Figure 4a. Therefore, the enhancement in the oscillator strength at higher concentrations of CH₃CN is attributed purely to the increased number density rather than to changes in the orientation factor (Figure 2a).

For the CH₃CN–water system, more CH₃CN molecules aggregate at the interface than do for the CH₃CN–CCl₄ and CH₃CN–CD₃CN systems (Figure 3). This is partly responsible for the enhanced oscillator strength at lower $x_{\text{CH}_3\text{CN}} (\leq 0.1)$ but cannot explain the attenuated oscillator strength when $x_{\text{CH}_3\text{CN}} > 0.1$, for which there are more CH₃CN molecules at the interface. The ordering and orientation of CH₃CN molecules should be considered to explain changes in the oscillator strength (eq 2). We propose that the concentration-dependent oscillator strength for the CH₃CN–water system is the result of two combined effects: surface number density and orientation factor.

When $x_{\text{CH}_3\text{CN}}$ is in the range of 0–0.1, the oscillator strength increases because of the enhancement in surface number density and the large orientation factor. However, the oscillator strength becomes attenuated because the increase in the surface number density cannot compensate for the reduction in the orientation factor when $x_{\text{CH}_3\text{CN}}$ is higher than 0.2 (Figure 2b).

In the CH₃CN–CCl₄ system, the rapid reduction of the oscillator strength is mainly caused by the attenuation of the orientation factor probably due to the random orientation of CH₃CN molecules at the interface. When $x_{\text{CH}_3\text{CN}}$ is less than 0.4, no detectable SFG signal intensity is observed despite the presence of a considerable concentration of CH₃CN at the air/liquid interface as calculated by eq 5 (Figure 2c).

Therefore, the unusual enhancement in SFG signal intensity for the CH₃CN–water system in Figures 1 and 2 at lower $x_{\text{CH}_3\text{CN}}$ is the result of the ordering and aggregation of CH₃CN molecules at the interface compared to the two other binary systems. The minimum bulk concentration of CH₃CN to produce observable SFG signal was as low as $x_{\text{CH}_3\text{CN}} \approx 0.0025$ for the CH₃CN–water mixture. This is in contrast to the case of the CH₃CN–CD₃CN and CH₃CN–CCl₄ solutions for which the minimum bulk mole fractions of CH₃CN needed to produce an SFG signal are about 0.05 and 0.4, respectively. We believe that this phenomenon is intimately related to the presence of hydrogen bonding between CH₃CN and water, but the role played by the hydrogen bonding in the ordering and aggregation of CH₃CN molecules at the interface is unclear at present.

We attempted to obtain more quantitative information on the molecular orientation of CH₃CN at the interface, although no spectral features for the CH(s) mode near 2944 cm^{−1} are found under the *sps* polarization combination (Figure 5). For the CH(s) mode of a methyl group with *C*_{3v} symmetry, it can be shown that

$$\left| \frac{\chi_{yyz}^{(2)}}{\chi_{yzy}^{(2)}} \right| = \left| \frac{\langle \cos \theta \rangle (1 + \gamma) - \langle \cos^3 \theta \rangle (1 - \gamma)}{[\langle \cos \theta \rangle - \langle \cos^3 \theta \rangle] (1 - \gamma)} \right| \quad (6)$$

where *x*, *y*, and *z* denote lab frame coordinates with the *z* axis along the surface normal, θ is the angle between the molecular axis of acetonitrile and the surface normal, and γ is the depolarization ratio of the methyl group.^{24–28} The SFG intensity ratio of the CH(s) mode with *ssp* and *sps* polarization combinations, I_{ssp}/I_{sps} , is proportional to $|\chi_{yyz}^{(2)}/\chi_{yzy}^{(2)}|^2$. More realistically, we expect that CH₃CN molecules have a range of possible orientations. To account for this, we introduce the orientation distribution function as a Gaussian, $P(\theta) = \exp[-(\theta - \theta_0)^2/(2\sigma^2)]$, where σ is the distribution width for tilting angle θ_0 with respect to the surface normal.

Figure 6 shows the calculated SFG intensity ratio of acetonitrile molecule, I_{ssp}/I_{sps} , as a function of tilting angle for various distribution widths ($\sigma = 0^\circ, 10^\circ, 20^\circ$, and 30°) using a depolarization ratio $\gamma = 2.3$.²⁹ Although there was no observable peak in the *sps* polarization combination for the CH(s) mode around 2944 cm^{−1} as shown in Figure 5, the noise level allowed us to set an upper limit on $A_{\text{CH(s),sps}}$. With a noise of 0.002 A.U. observed in Figure 5, we obtain that $A_{\text{CH(s),sps}} < 0.45$ A.U. in the *sps* polarization combination. As shown in Figure 2, the oscillation strength $A_{\text{CH(s),ssp}}$ obtained from data fitting equals 10.75 A.U. for neat CH₃CN. Therefore, eq 1 gives $I_{ssp}/I_{sps} > 500$ for neat CH₃CN. If we assume that the molecular orientation exhibits a δ function distribution (or $\sigma = 0^\circ$), from eq 6 and the Fresnel factor, we found that the tilting angle θ_0 must be less than 28° (see lines 1 and a in Figure 6). Similarly, if we

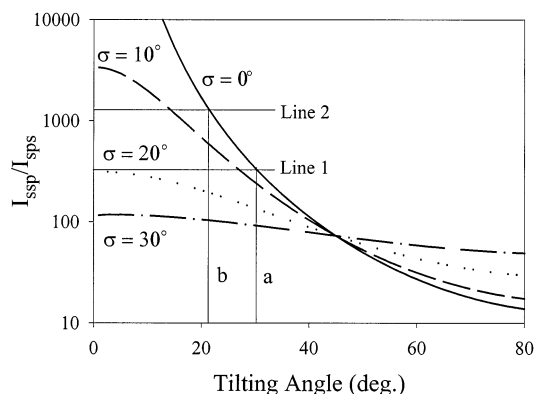


Figure 6. Calculated I_{ssp}/I_{sps} of methyl group in acetonitrile as a function of tilting angle θ_0 and angle distribution σ .

assume that all CH_3CN molecules are perpendicular to the surface ($\theta_0 = 0^\circ$), σ must be less than 18° .

For the CH_3CN –water system, I_{ssp}/I_{sps} is larger than 1200 when $x_{\text{CH}_3\text{CN}}$ is 0.1 (see Figures 1 and 5). Similarly, θ_0 must be less than 23° for $\sigma = 0^\circ$ (see lines 2 and b in Figure 6) and σ must be less than 13° for $\theta_0 = 0^\circ$. When $x_{\text{CH}_3\text{CN}}$ is greater than 0.2, CH_3CN molecules become gradually tilted (see line b in Figure 4). This result shows that the orientation of CH_3CN in the CH_3CN –water system is slightly different from that proposed by Zhang et al. in view of tilting angle and bulk concentration where structural transitions occur.^{12–14} It was proposed that CH_3CN tilts about 40° with respect to the surface normal and abruptly changes by 70° when $x_{\text{CH}_3\text{CN}}$ is 0.07.

CH_3CN molecules in the CH_3CN – CCl_4 system are expected to be more tilted and randomly oriented than those in neat CH_3CN with lowering CH_3CN concentration, as indicated by the attenuated orientation factor in Figure 4c. However, the tilting angle is not in the range to produce observable SFG spectral evidence of the CH(a) and CH(s) modes under the *ssp* and *sps* polarization combinations, respectively.

Conclusions

We investigated the structure and dynamics of CH_3CN at the air/binary liquid interface with changing bulk compositions using SFG vibrational spectroscopy. Compared to the reference mixtures of CH_3CN – CD_3CN , an enhancement in the ordering of CH_3CN molecules was observed for the CH_3CN –water solution, presumably because of hydrogen bonding. In contrast, CH_3CN molecules in the binary CH_3CN – CCl_4 mixtures are less ordered and more tilted. The results presented here provide a good example of how the ordering and orientation of CH_3CN molecules at the air/liquid interface is affected by chemical environments, which is dictated by the nature and concentration of the coexisting component in the binary solution.

Acknowledgment. This work was supported by the Director, Office of Science, Office of Basic Energy Sciences, Division

of Materials Sciences and Engineering, of the U. S. Department of Energy under Contract No. DE-AC03-76SF00098.

Note Added after ASAP Posting. This article was released ASAP on 1/17/2003 with an error in the Experimental Section, three sentences after eq 3. To correct the error in this sentence (which begins with “In eq 3”) π was deleted. An error also appeared in the Discussion, after eq 6, in the paragraph beginning “Figure 6 shows”. To correct the error in the fourth sentence (which begins with “As shown in”) $A_{\text{CH(s),sps}}$ was replaced with $A_{\text{CH(s),ssp}}$. The correct version was posted on 1/22/2003.

References and Notes

- (1) Benjamin, I. *Chem. Rev.* **1996**, *96*, 1449–1476.
- (2) Eisenthal, K. B. *Chem. Rev.* **1996**, *96*, 1343–1360.
- (3) Miranda, P. B.; Shen, Y. R. *J. Phys. Chem. B* **1999**, *103*, 3292–3307.
- (4) Kuzmenko, I.; Rapaport, H.; Kjaer, K.; Als-Nielsen, J.; Weissbuch, I.; Lahav, M.; Leiserowitz, L. *Chem. Rev.* **2001**, *101*, 1659–1696.
- (5) Ulman, A. *Chem. Rev.* **1996**, *96*, 1533–1554.
- (6) Kim, J.; Cremer, P. S. *J. Am. Chem. Soc.* **2000**, *122*, 12371–12372.
- (7) Kim, J.; Kim, G.; Cremer, P. S. *J. Am. Chem. Soc.* **2002**, *124*, 8751–8756.
- (8) Kim, J.; Chou, K. C.; Somorjai, G. A. *J. Phys. Chem. B* **2002**, *106*, 9198–9200.
- (9) Richmond, G. L. *Anal. Chem.* **1997**, *69*, 536A–543A.
- (10) Gracias, D. H.; Chen, Z.; Shen, Y. R.; Somorjai, G. A. *Acc. Chem. Res.* **1999**, *32*, 930–940.
- (11) Wang, J.; Woodcock, S. E.; Buck, S. M.; Chen, C.; Chen, Z. *J. Am. Chem. Soc.* **2001**, *123*, 9470–9471.
- (12) Wang, H.; Borguet, E.; Yan, E. C. Y.; Zhang, D.; Gutow, J. H.; Eisenthal, K. B. *Langmuir* **1998**, *14*, 1472–1477.
- (13) Zhang, D.; Gutow, J. H.; Eisenthal, K. B.; Heinz, T. F. *J. Chem. Phys.* **1993**, *98*, 5099–5101.
- (14) Zhang, D.; Gutow, J. H.; Eisenthal, K. B. *J. Chem. Soc., Faraday Trans.* **1996**, *92*, 539–543.
- (15) Shen, Y. R. *Nature* **1989**, *337*, 519–525.
- (16) Shen, Y. R. *Surf. Sci.* **1994**, *299/300*, 551–562.
- (17) Grundy, W. M.; Schmitt, B. J. *Geophys. Res.* **1998**, *103*, 25809–25825. The infrared absorption coefficient of acetonitrile, 350 cm^{-1} , was measured in our laboratory.
- (18) Somorjai, G. A. *Introduction to Surface Chemistry and Catalysis*; John Wiley & Sons: New York, 1994.
- (19) Kipling, J. J. *J. Colloid Sci.* **1963**, *18*, 502–511.
- (20) Guggenheim, E. A.; Adam, N. K. *Proc. R. Soc. London* **1933**, *A139*, 218–236.
- (21) Wolfrum, K.; Graener, H.; Laubereau, A. *Chem. Phys. Lett.* **1993**, *213*, 41–46.
- (22) Cheong, W. J.; Carr, P. W. *J. Liq. Chromatogr.* **1987**, *10*, 561–581.
- (23) Teixeira, P. I. C.; Almeida, B. S.; Telo da Gama, M. M.; Rueda, J. A.; Rubio, R. G. *J. Phys. Chem.* **1992**, *96*, 8488–8497.
- (24) Zhuang, X.; Miranda, P. B.; Kim, D.; Shen, Y. R. *Phys. Rev. B* **1999**, *59*, 12632–12640.
- (25) Wei, X.; Hong, S.-C.; Zhuang, X.; Goto, T.; Shen, Y. R. *Phys. Rev. E* **2000**, *62*, 5160–5172.
- (26) Hirose, C.; Akamatsu, N.; Domen, K. *Appl. Spectrosc.* **1992**, *46*, 1051–1072.
- (27) Hirose, C.; Akamatsu, N.; Domen, K. *J. Chem. Phys.* **1992**, *96*, 997–1004.
- (28) Hirose, C.; Yamamoto, H.; Akamatsu, N.; Domen, K. *J. Phys. Chem.* **1993**, *97*, 10064–10069.
- (29) Zhang, D.; Gutow, J.; Eisenthal, K. B. *J. Phys. Chem.* **1994**, *98*, 13729–13734.